Phys Chem Minerals (1992) 19:106–120

PHYSICS AND CHEMISTRY OF MINERALS

High-Temperature Thermal Expansion and Elasticity of Calcium-Rich Garnets

Donald G. Isaak, Orson L. Anderson, and Hitoshi Oda

Institute of Geophysics and Planetary Physics, University of California, Los Angeles, CA 90024, USA

Received July 29, 1991 / Revised, accepted January 20, 1992

Abstract. We present new high temperature elasticity data on two grossular garnet specimens. One specimen is single-crystal, of nearly endmember grossular, the other is polycrystalline with about 22% molar andradite. Our data extend the high temperature regime for which any garnet elasticity data are available from 1000 to 1350 K and the compositional range of temperature data to near endmember grossular. We also present new data on the thermal expansivity of calcium-rich garnet. We find virtually no discernable differences in the temperature T derivatives at ambient conditions of the isotropic bulk K_S and shear μ moduli when comparing our results between these two specimens. These calcium-rich garnets have the lowest values of $|(\partial K_S/\partial T)_P| = (1.47, 1.49) \times 10^{-2}$ GPa/K, and among the highest values of $|(\partial \mu/\partial T)_P| = 1.25 \times 10^{-2}$ GPa/K, when compared with other garnets. Small, but measurable, nonlinear temperature dependences of most of the elastic moduli are observed. Several dimensionless parameters are computed with the new data and used to illustrate the effects of different assumptions on elastic equations of state extrapolated to high temperatures. We discuss how dimensionless parameters and other systematic considerations can be useful in estimating the temperature dependence of some properties of garnet phases for which temperature data are not yet available. While we believe it is premature to quantitatively predict the temperature variation of K_S and μ for majorite garnets, our results have bearing on the amount of diopside required to explain the shear velocity gradients in Earth's transition zone.

Introduction

Garnet is an important mineral in Earth's mantle. Most current petrological models, whether olivine-rich or poor, suggest that the upper mantle contains about 13–15 vol% garnet (Duffy and Anderson 1989). Furthermore it is likely that pyroxene transforms to a garnet structure (majorite) under the pressure and temperature conditions of Earth's transition zone, and a gradual transformation of calcium and aluminum-rich clinopyroxene has been used in attempting to explain the high velocity gradients throughout the transition zone (Bass and Anderson 1984). Thus an accurate description of the chemistry and structure of Earth's mantle necessarily implies reliable information regarding the elastic properties of garnet throughout the pressure, temperature, and chemical conditions of the mantle.

Much recent work has been done to characterize, in particular, how the elastic properties of pyralspite, uvarovite, and andradite garnets depend on the chemical composition (Wang and Simmons 1974; Weaver et al. 1976; Leitner et al. 1980; Babuska et al. 1978; Bass 1986; O'Neill et al. 1989; Bass 1989; O'Neill et al. 1991). Recent Brillioun spectroscopy has also provided new elasticity data on majorite garnets at ambient conditions (Bass and Kanzaki 1990; Yeganeh-Haeri et al. 1990). Relatively fewer data are available on the temperature dependence of the elastic properties of garnets, which is the focus of our study. The temperature dependence of elasticity has been reported for almandine-spessartine $(Fe_{0.52}, Mn_{0.46}, Ca_{0.01})_3Al_2Si_3O_{12}$ (Isaak and Graham 1976), pyrope-almandine $(Mg_{0.61}, Fe_{0.36}, Ca_{0.02})_3Al_2Si_3O_{12}$ (Bonczar and Graham 1977), and three specimens of predominantly pyrope and almandine (Sumino and Nishizawa 1978). All of these derivatives are evaluated at ambient conditions based on data obtained over the temperature range 300–475 K. Two earlier sets of data on temperature derivatives of elasticity (Reddy and Bhimasenachar 1964; Soga 1964) include some values which appear to be anomalous (Sumino and Nishizawa 1978). Furthermore, there is no mention of the composition in the paper by Reddy and Bhimasenachar (1964).

More recently Suzuki and Anderson (1983) extended the temperature range for which data have been obtained out to 1000 K using one of the pyrope-almandine specimens (SN78) reported on by Sumino and Nishizawa

(1978). Here we further extend the temperature range to beyond 1300 K and report elasticity data on two grossular specimens, one being nearly endmember $Ca_3Al_2Si_3O_{12}$. The high temperatures attained in our work provide a firmer basis for extrapolating to temperature conditions in the transition zone since the effects of nonlinear temperature dependence of elasticity are better assessed. We evaluate various thermal equations of state which have been used to extrapolate beyond the range of measurements.

Our experiments extend the compositional regime to include calcium-rich garnets for which data on the elastic moduli as a function of temperature are now available. Extending the compositional range over which this data are available is important in order to understand the systematics which relate dimensionless parameters to temperature derivatives of the isotropic bulk and shear moduli. Accurate application of these systematics to high-pressure mineral phases in the mantle require more information on the effects of chemical variations on the high temperature properties within a solid series. Since these dimensionless parameters depend not only on the elastic moduli but also on the thermal expansion, and since there is evidence that the thermal expansion data reported by Skinner (1956) on several garnets are systematically low, we also present new thermal expansion data on a calcium-rich garnet.

These data also provide a chance to assess the possibility of retrieving good quality elasticity data on a polycrystalline specimen at high temperature since one of the specimens we used was polycrystalline. This study is a first step in consideration of further experiments to obtain high-temperature elasticity data on any polycrystalline high-pressure phase made from compressed powders (Gwanmesia et al. 1990a). To date only the pressure dependence of the wave velocities have been measured on any high-pressure phase (β-olivine) made from powders (Gwanmesia et al. 1990b). Eventhough our specimens are stable at ambient pressure, whereas quenched high-pressure phases are metastable, it must be determined first whether adequate quality of temperature data for a stable polycrystalline specimen can be retrieved, before attempting similar experiments with high pressure phases fabricated from powder.

Specimen Description

Polycrystalline Grossular-Andradite (GR-2B)

We used two natural garnet specimens in our experiments. One specimen was polycrystalline, and the other single-crystal. The polycrystalline specimen, GR-2B used by Babuska et al. (1978) in their measurements of elasticity of garnets at room temperature, is approximately 76% grossular and 22% andradite, with very small amounts of spessartine and pyrope. Preliminary data on the temperature dependence of the isotropic elastic moduli were also reported on this specimen (Isaak and Anderson 1987). Since that time we obtained a new set of elasticity data on GR-2B to higher temperature, 1250 K compared to 989 K, and used nearly twice as many modal frequencies, which produce some small differences between our present results and our earlier measurements. Details of the chemical composition from the analysis of Babuska et al. (1978) on specimen GR-2B are given in Table 1. Babuska et al. (1978) used a centrifugal technique to measure the density ρ of this polycrystalline specimen and found $\rho = 3.667 \pm 0.003$ gm cm^{-3}, which is only slightly larger than the calculated density of 3.661 g cm^{-3} found by using the molar percents and the garnet endmember density data of Skinner (1956). The close agreement between the measured and calculated density of this polycrystalline specimen indicates that no significant porosity is present. The cut specimen has dimensions 3.667 ± 0.005, 3.714 ± 0.004, and 3.839 ± 0.004 mm.

Table 1. Garnet Chemical Analysis

Mass composition of oxides		
Oxides	mass%	
	GR-2B[a]	GGD
SiO_2	38.20	39.97
TiO_2	0.26	0.55
Al_2O_3	17.13	22.20
Cr_2O_3	–	–
Fe_2O_3	7.55	–
FeO	trace	0.18
MnO	0.57	0.16
MgO	0.14	0.33
CaO	34.85	36.60
Modal endmember composition		
Garnet component	molar%	
	GR-2B[1]	GGD
almandine, $Fe_3Al_2Si_3O_{12}$	0.0	0.37
andradite, $Ca_3[Ti, Fe^{+3}]_2Si_3O_{12}$	22.1	1.56
grossular, $Ca_3Al_2Si_3O_{12}$	76.1	96.53
pyrope, $Mg_3Al_2Si_3O_{12}$	–	1.20
spessartine, $Mn_3Al_2Si_3O_{12}$	1.3	0.33

[a] Babuska et al. (1978)

Single-Crystal Grossular (GGD)

We obtained this single-crystal garnet specimen from J. Bass, University of Illinois. Results of the electron microprobe (EMP) for the specimen GGD (Table 2) show it to be almost 97% pure grossular, thus very close to endmember composition. By assuming that the small amount of Ti present is in the trivalent Y site ($X_3^{+2}Y_2^{+3}Si_3O_{12}$) (Papike 1987), there is good chemical balance in this site from the sum of the Al and Ti ions. All Ca, Mg, and the very minor amounts of Fe and Mn present are then assumed to occupy the divalent X site (Papike 1987) in the construction of the molar percents of Table 1 for this specimen.

Table 2. Thermal Expansion of Grossular Garnet

T K	Y_L(obs) 10^{-3}	Y_V(obs) 10^{-2}	Y_V(cal)[a] 10^{-2}	α GR-2B[b] $10^{-6}\,K^{-1}$	α grossular[c] $10^{-6}\,K^{-1}$
300	0.050	0.013	0.014	20.2	19.2
350	0.398	0.119	0.120	22.1	21.3
400	0.779	0.234	0.234	23.5	22.8
450	1.177	0.354	0.355	24.5	24.0
500	1.595	0.479	0.480	25.3	24.9
550	2.025	0.609	0.609	26.0	25.6
600	2.463	0.741	0.741	26.5	26.1
650	2.911	0.876	0.876	27.0	26.6
700	3.366	1.013	1.013	27.3	27.1
750	3.823	1.151	1.152	27.7	27.4
800	4.285	1.291	1.293	28.0	27.8
850	4.760	1.434	1.435	28.2	28.1
900	5.236	1.579	1.579	28.5	28.3
950	5.716	1.725	1.725	28.7	28.6
1000	6.198	1.871	1.871	28.9	28.8
1050			2.019	29.1	29.0
1100			2.169	29.3	29.2
1150			2.319	29.5	29.5
1200			2.471	29.7	29.7
1250			2.624	29.9	29.9
1300			2.777	30.1	30.0
1350			2.933	30.2	30.2
1400			3.089	30.4	30.4
1500			3.404	30.8	30.8
1600			3.725	31.1	31.2
1700			4.050	31.4	31.6
1800			4.379	31.8	32.0
1900			4.713	32.2	32.3
2000			5.053	32.5	32.7

Uncertainty in α is estimated at 2%

[a] Calculated from (3) and (4) using the best fit parameters $Q_0 = 17.587$ MJ mole^{-1}, $\theta_D = 821.0$ K, $k = 1.681$, and $a_V = 0.0026$ found from observed $Y_V(T)$ for $T \leqq 1000$ K

[b] $\alpha = (1/V)(\partial V/\partial T)_P$ from analytic differentiation of (3)

[c] α for endmember grossular. Found from present results with added assumption that relative difference between andradite and grossular α is that given by Skinner (1956)

We did not obtain the bulk density of this specimen by immersion because during one high temperature run the specimen melted (between 1400–1450 K). However prior to melting we had carefully measured the mass of the specimen on two digital balances, each having 10 μg precision. From these measurements of mass, together with the measured lengths, we found the density to be 3.592 ± 0.006 g cm^{-3}. The calculated density is 3.603 g cm^{-3} from the endmember compositions, together with the molar volumes and densities given by Skinner (1956). This calculated value is near, but slightly outside, the range of density found by dividing the measured mass by volume. In our experience, using the measured mass and volume to obtain the density tends to slightly underestimate the actual density, by up to about 0.01 g cm^{-3}, since the volume found in this way is usually a little too high. Thus, 3.592 and 3.603 g cm^{-3} are taken to be respective, lower and upper bounds to the actual sample density, and the average value of 3.597 ± 0.006 g cm^{-3} is used in our analysis. All errors in the tabulated elasticity values propagate this uncertainty in ρ.

New Garnet Thermal Expansion Measurements

Thermal expansion data on grossular garnet is included in the garnet endmember data in the work of Skinner (1956). However, more recent thermal expansion data on pyrope-almandine (Suzuki and Anderson 1983) and almandine-pyrope (Soga 1967) are 10–15% higher than found from the pyrope and almandine endmember data of Skinner (1956). In view of these discrepancies we made new thermal expansion measurements for grossular garnet, using a horizontal differential dilatometer (Theta Industries, Model Dilametric IR) to measure the expansion of the longest edge of specimen GR-2B from room temperature to nearly 1000 K. The dilatometer is a double pushrod type in which the difference in length, as heating occurs, between the sample and a reference material is recorded by a calibrated linearly variable displacement transformer (LVDT). We used single-crystal sapphire (Theta Industries), cut to approximately the same length as the garnet edge being investigated, as the reference material. Sapphire is an ideal reference material in this situation since its expansivity is not only well characterized, but also is near that of garnet.

We calibrated the LVDT by measuring the voltage output when several steel gauges, with thicknesses varying from 0.078–0.499 mm, were inserted in one of the cells. The DVDT response was quite linear over this range in displacements. Since the differential displacements between garnet and sapphire during our experiments were less than 0.078 mm, we further tested our calibration using two reference materials, sapphire and fused silica, by heating them up to 650 K. Comparing the results of these tests with standard tables for the expansion of sapphire and fused silica (Theta Industries) indicates that the uncertainty introduced into our calculated volume coefficient of thermal expansion, due to errors in the absolute calibration, is about 1%. At low temperatures, 300–400 K, the coefficient of expansion is relatively smaller and the percent error is a little larger.

In obtaining the expansivity data we made four separate temperature runs from 293–998 K, interchanging the position of the garnet and sapphire after each run. Thus, in runs 1 and 3 the sapphire and garnet were in the same positions. In runs 2 and 4 their positions were interchanged with those of runs 1 and 3. Figure 1 (lower curve) includes the primary linear expansivity data, $Y_L(T) = [L(T) - L(T_{ref})]/L(T_{ref})$, where T_{ref} is ambient temperature and the average of the four runs at each temperature is the value plotted. We found very little difference in measured expansivity when comparing the data obtained for the two runs when specimen GR-2B was in the same position. That is when comparing run 1 with run 3, and in comparing run 2 with run 4, the difference in expansivity is less than 1%. When the positions of the garnet and sapphire are reversed (runs 1 and 3 compared to runs 2 and 4) the difference in measured expansivity is 4% at the highest temperature of 998 K, and less at lower temperatures. This baseline effect is the predominant source of uncertainty, but its effect on the results tends to cancel out by interchanging the specimen and sapphire positions and taking the aver-

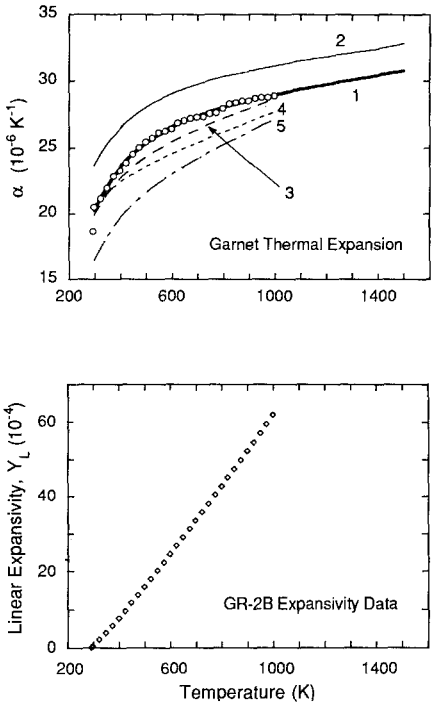

Fig. 1. Volume coefficient of thermal expansion for garnets (*upper curve*): (1) grossular-andradite (GR-2B) of present study; (2) pyrope-almandine (Suzuki and Anderson 1983); (3) pyrope (Skinner 1956); (4) andradite (Skinner 1956); and (5) grossular (Skinner 1956). The symbols show α of specimen GR-2B obtained by (6), and the *thick solid line* is from application of (1–5) described in text. The lower plot shows the linear expansivity Y_L from which the top GR-2B α curves were obtained

age $Y_L(T)$ values. We estimate the final volume expansivity results are accurate to approximately 2% over the temperature range of 293–998 K.

We used the method described by Suzuki et al. (1979) to obtain the volume coefficient of thermal expansion from the original expansivity $Y_V(T)$ data, where

$$Y_V(T)=\frac{V(T)-V(T_{\mathrm{ref}})}{V(T_{\mathrm{ref}})} \tag{1}$$

and is related to the observed $Y_L(T)$ by

$$Y_V(T)=3\,Y_L(T)+3\,Y_L^2(T)+Y_L^3(T). \tag{2}$$

In (1) and (2), $V(T)$ refers to the volume at some elevated temperature, and $V(T_{\mathrm{ref}})$ is the volume at an ambient reference temperature. In this method the Mie-Grüneisen equation of state is assumed to be represented by a Taylor series expansion to second order with respect to the volume change $\Delta=V-V_0$, where V_0 is the volume at 0 K (Suzuki 1975). The procedure described by Suzuki et al. (1979) treats the second order expansion term exactly, in which case the expansivity $Y_V(T)$ can be written as

$$Y_V(T)=\frac{1+2k-\sqrt{1-4kE(\theta_D,T)/Q_0}}{2k\,a_V}-1. \tag{3}$$

In (3), $k=(K_0'-1)/2$, K_0' being the pressure derivative $(\partial K/\partial P)_0$ of the bulk modulus K at 0 K, $Q_0=K_0\,V_0/\gamma$, where γ is the Grüneisen parameter discussed in a later section, and $a_V=V(T_{\mathrm{ref}})/V_0$. The nought subscripts refer to conditions at 0 K. Our reference temperature T_{ref} is 293 K. In (3), θ_D is the Debye temperature and $E(T,\theta_D)$ is the thermal energy given by

$$E(T,\theta_D)=9\,pRT\left(\frac{T}{\theta_D}\right)^3\int_0^{\theta_D/T}\frac{z^3}{e^z-1}\,dz \tag{4}$$

where p is the number of atoms in the molecular formula and R is the gas constant. From the representation of $Y_V(T)$ given by (3) we used a least squares fit with the observed $Y_V(T)$ data to determine the parameters Q_0, θ_D, k, and a_V. Analytical differentiation of $Y_V(T)$ with respect to T, using the best fit Q_0, θ_D, k, and α_V values, then is done to find the thermodynamic volume coefficient of thermal expansion $\alpha_V=\alpha=(1/V)(\partial V/\partial T)_P$ by

$$\alpha=\frac{\dfrac{\partial}{\partial T}\left[V(T_{\mathrm{ref}})(1+Y_V)\right]_P}{V(T_{\mathrm{ref}})(1+Y_V)}=\left(\frac{1}{1+Y_V}\right)\left(\frac{\partial Y_V}{\partial T}\right)_P. \tag{5}$$

In Table 2 we list the observed Y_L, and the corresponding Y_V values found from (2), in steps of 50°. We recorded the expansivity data at 293 K, and then in steps of 25° starting at 298 K (i.e., at 298, 323, 348, 373 K and so on up to 998 K). The observed Y_L and Y_V values shown in Table 2 at regular increments represent a small interpolative adjustment of two degrees. Table 2 also shows the Y_V and α calculated from the measured expansivity data using the procedure described by (1–5) above. The final best fit parameters used in (3) and (4) are $Q_0=17.587$ MJ/mole, $\theta_D=821.0$ K, $k=1.681$, and $a_V=0.0026$. The last column in Table 2 gives new estimated values for α of endmember grossular from our new data on GR-2B, with the assumption that the percent difference in α between andradite and grossular is that given by Skinner (1956).

We show results for the α values found for GR-2B, using the analysis of (1–5), by the solid line in Fig. 1. Included in Fig. 1 (circular symbols) are values calculated for α by numerical differentiation of the $Y_V(T)$ data directly according to

$$\alpha=\frac{Y_V(T+\Delta T)-Y_V(T-\Delta T)}{2\Delta T[1+Y_V(T)]} \tag{6}$$

using steps of 25° for ΔT.

When we compare the new α data on the GR-2B garnet specimen with the previous grossular and andradite data of Skinner (1956) (see Fig. 1), we find a decided upward shift over the earlier results of Skinner. We find that α calculated for a garnet with GR-2B composition from the endmember data of Skinner (1956) to be lower by 16% at 300 K, and by 7% at 950 K, than found from our new data. These differences are outside the estimated error bars (2%) of our results, and are similar to the higher α values found by Suzuki and Anderson (1983) for pyrope-almandine and by Soga (1967) for almandine-pyrope, when compared with values calculated from the endmember data of Skinner (1956). Figure 1 includes the

data of Suzuki and Anderson (1983) on their predominantly pyrope specimen and the results on pyrope from Skinner (1956). The quality of the GR-2B specimen, as evidenced by the good agreement in measured and calculated densities, is such that porosity is apparently not a noticeable problem with this polycrystalline specimen. We do not know the reasons for the differences between our results and those of Skinner (1956). However, our results along with those of Suzuki and Anderson (1983) and Soga (1967), taken as a whole are evidence that the α obtained by Skinner (1956) for endmember garnets are somewhat low.

We also note that the effect of substituting Ca for Mg in garnet, which is a silicate oxide, has a similar effect on α as in the oxides CaO and MgO at elevated temperature. We compared α for CaO, calculated from the expansivity data recommended by Touloukian (1977) using the Suzuki method described above (H. Oda, unpublished work), with the MgO α data of Suzuki (1975). Although CaO and MgO have nearly the same value for α at room temperature, at 500 K the value of α for MgO is about 6% geater than for CaO, and this difference increases to 15% at 1200 K. Over this same temperature span of 500–1200 K, α for the pyrope-almandine used by Suzuki and Anderson (1983) is 7–10% greater than that of the grossular-andradite GR-2B.

Elasticity Experimental Procedure

We used the rectangular parallelepiped resonance (RPR) method to measure the adiabatic elastic moduli from room temperature to 1250 K (GR-2B) and 1350 K (GGD). The RPR technique has recently been used to measure the high temperature elastic moduli C_{ij}^S, for a variety of minerals: corundum (Goto et al. 1989); forsterite (Isaak et al. 1989a); MgO (Isaak et al. 1989b); and natural olivine (Isaak 1992). In this method the temperature dependences of the natural resonant frequencies of an orientated specimen, cut in the shape of a rectangular parallelepiped along the crystallographic axes, are observed. At each temperature the measured frequencies, together with the known density and edge lengths of the cut specimen, are used to calculate in an inverse manner the adiabatic elastic moduli. We follow the data reduction scheme described by Ohno (1976) and by Sumino et al. (1976) in obtaining the elastic moduli from the observed resonant modes.

Suzuki and Anderson (1983) used the RPR technique to measure the C_{ij}^S of pyrope-almandine to 1000 K. Here we used an apparatus equipped with buffer rods (Goto and Anderson 1988), which was previously used to retrieve data on corundum to 1825 K (Goto et al. 1989) and on forsterite to 1700 K (Isaak et al. 1989a). In our measurements the resonant signals were unobservable at temperatures higher than 1250 and 1350 K, respectively, for GR-2B and GGD. Thus the specimens, and not the apparatus, were the factors limiting the span of temperatures over which we obtained data. The frequency data were checked at a few temperature points during cooling and/or reheating after these highest temperatures were obtained, and found to be reproducible within the reported errors. These checks were done to ensure that no permanent changes occured in the specimens upon the heating during the runs on which our final C_{ij}^S are based. It is especially noteworthy that virtually no change in the room temperature frequency spectrum was observed for specimen GR-2B after it had been heated to 1250+ K. We did not control the atmosphere on this specimen which contains appreciable iron. There was a concern that some of the iron could have oxidized. However, by careful measurement of the resonant spectrum both before, and after, heating we can rule out the possibility that a chemical change in this specimen at high T affected the data. Although specimen GGD melted upon heating beyond 1400 K as mentioned above, we had previously verified the reproducibility of the data to 1350 K.

We observed the lowest 37 resonant modes of GR-2B, and 15 of the 22 lowest modes of GGD, each at intervals of 50 K over their respective temperature ranges. We did not use all of the lowest 22 modes of GGD because the amplitudes of several of these modes were quite small. In our data reduction for the single-crystal specimen GGD we determined the three independent adiabatic elastic moduli $K_S=(1/3)(C_{11}^S+2C_{12}^S)$, $C_S=(1/2)(C_{11}^S-C_{12}^S)$, and C_{44} directly from the frequency data at each temperature. The C_{11}^S and C_{12}^S moduli, and their errors, were then obtained from K_S and C_S. We used a similar scheme in the data reduction of the polycrystalline specimen GR-2B, in which case C_S and C_{44} are viewed as effective shear moduli in a polycrystalline isotropic body. The degree to which these two effective moduli are not equal to each other (<1% at all temperatures) is representative of the nonisotropic properties of the polycrystalline specimen.

Results

The results of our new elasticity data for specimens GR-2B and GGD are shown in Figs. 2–6. We tabulate several isotropic bulk properties, including the wave velocities, in Tables 3a, b throughout the temperature range of our experiments. The errors listed at representative temperatures in Tables 3a, b, and also those indicated in Fig. 2–6, include the uncertainty in ρ as well as the standard deviations of the measured frequencies. The quantity K_T in Tables 3a, b is the isothermal bulk modulus given by

$$K_T=\frac{K_S}{1+\alpha\gamma T} \tag{7}$$

where γ is the Grüneisen parameter

$$\gamma=\frac{\alpha K_S}{\rho C_P}. \tag{8}$$

The isotropic shear modulus μ is calculated by the average of the Hashin-Shtrikman (1962) upper and lower bounds, where the listed errors include these bounds. The isotropic wave velocities, V_p and V_s, are the respec-

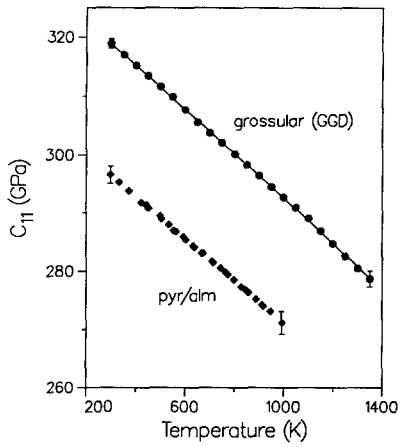

Fig. 2. Temperature variation of modulus C_{11}^S of grossular GGD. *Solid line* is from fit coefficients given in Table 5 using (12). Also shown are the pyrope-almandine (pyr/alm) data of Suzuki and Anderson (1983). Representative errors bars are included at two temperatures

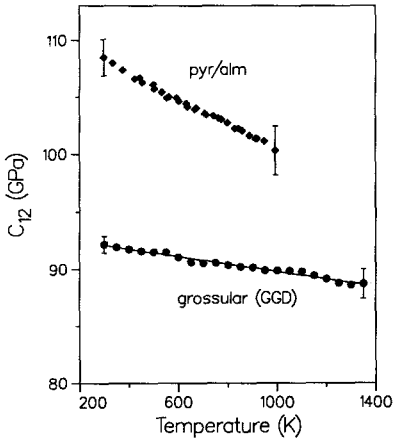

Fig. 3. Temperature variation of modulus C_{12}^S of grossular GGD. *Solid line* is from fit coefficients given in Table 5 using (12). Also shown are the pyrope-almandine (pyr/alm) data of Suzuki and Anderson (1983). Representative errors bars are included at two temperatures

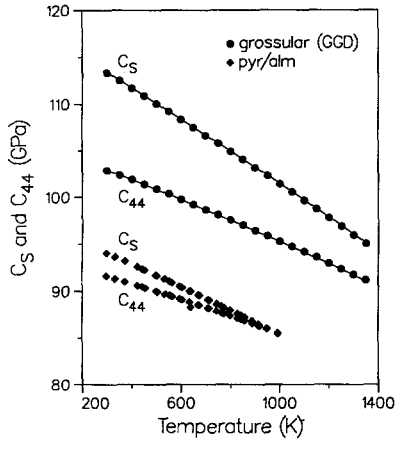

Fig. 4. Temperature variations of the shear moduli C_S and C_{44} of grossular GGD. *Solid lines* are from fit coefficients given in Table 5 using (12). Also shown are the pyrope-almandine (pyr/alm) data of Suzuki and Anderson (1983). Errors are within the size of the symbols

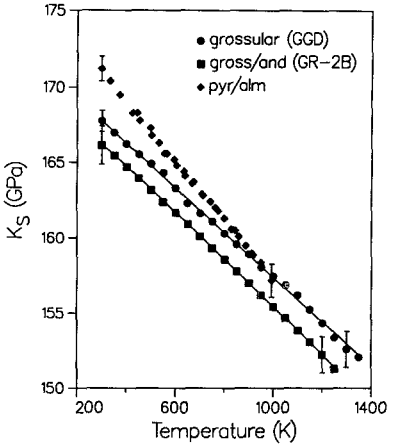

Fig. 5. Temperature variation of the isotropic adiabatic bulk moduli K_S for garnet specimens GGD and GR-2B studied here, and pyrope-almandine (pyr/alm) (Suzuki and Anderson 1983). *Solid lines* are from fit coefficients given in Table 5 using (12). Representative errors bars are included at two temperatures

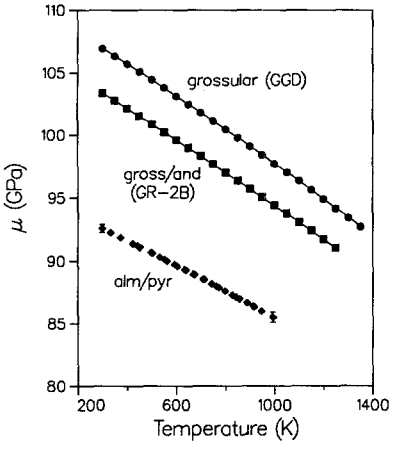

Fig. 6. Temperature variation of the isotropic shear moduli μ for garnet specimens GGD and GR-2B studied here, and pyrope-almandine (pyr/alm) (Suzuki and Anderson 1983). Solid lines are from fit coefficients given in Table 5 using (12). Errors, where not shown, are within the size of the symbols

tive compressional and shear wave velocities obtained by

$$V_p = \left(\frac{K_S + (4/3)\mu}{\rho}\right)^{1/2} \tag{9}$$

and

$$V_s = \left(\frac{\mu}{\rho}\right)^{1/2}. \tag{10}$$

The acoustic Debye temperature θ_D can then be calculated using V_p and V_s from

$$\theta_D = 251.45 \left(\frac{\rho}{m}\right)^{1/2} \left[\frac{1}{3}\left(V_p^{-3} + 2V_s^{-3}\right)\right]^{-1/3} \tag{11}$$

where m is the mean atomic mass.

We also compare our results with other garnet elasticity data at 300 K (Table 4), and with temperature deriva-

Table 3a. Measured Thermodynamic Properties of Grossular-Andradite Garnet (GR-2B) to 1250 K

T K	ρ g cm^{-3}	C_P[a] J (g K)$^{-1}$	K_S GPa	K_T GPa	μ GPa	V_p km s^{-1}	V_s km s^{-1}	θ_D K
300	3.667±0.003	0.734	166.15±1.28	164.9±1.3	103.38±0.24	9.105±0.020	5.310±0.006	804±1
350	3.663	0.807	165.46	163.9	102.78	9.088	5.297	802
400	3.659	0.865	164.69	162.8	102.15	9.068	5.284	800
450	3.654	0.912	163.92	161.7	101.51	9.050	5.271	797
500	3.650	0.948	163.17	160.7	100.88	9.031	5.257	795
550	3.645	0.977	162.36	159.7	100.23	9.011	5.244	793
600	3.640	1.000	161.67	158.7	99.60	8.995	5.231	790
650	3.635	1.018	160.90	157.7	98.97	8.976	5.218	788
700	3.630	1.033	160.11	156.6	98.33	8.957	5.205	786
750	3.626	1.045	159.33	155.6	97.68	8.938	5.190	783
800	3.620±0.004	1.056	158.58±1.24	154.6±1.2	97.02±0.23	8.919±0.020	5.177±0.006	780±1
850	3.615	1.066	157.80	153.5	96.37	8.899	5.163	778
900	3.610	1.075	157.02	152.5	95.72	8.880	5.149	776
950	3.605	1.083	156.21	151.5	95.06	8.860	5.135	774
1000	3.600	1.093	155.44	150.5	94.42	8.840	5.121	771
1050	3.595	1.102	154.67	149.5	93.76	8.820	5.107	769
1100	3.589	1.113	153.83	148.4	93.05	8.800	5.093	767
1150	3.584	1.124	153.05	147.4	92.42	8.780	5.078	763
1200	3.579±0.005	1.137	152.23±1.20	146.4±1.2	91.74±0.22	8.759±0.020	5.063±0.006	761±1
1250	3.574	1.151	151.27	145.3	91.06	8.734	5.048	758

T: Temperature. ρ: Density. C_P: Specific heat capacity at constant pressure. K_S and K_T: Adiabatic and isothermal bulk (isotropic) moduli. μ: Isotropic shear modulus. V_p and V_s: Isotropic compressional and shear wave velocities. θ_D: Debye temperature
[a] Krupka et al. (1979)

Table 3b. Measured Thermodynamic Properties of Grossular Garnet (GGD) to 1350 K

T K	ρ g cm^{-3}	C_P[a] J (g K)$^{-1}$	K_S GPa	K_T GPa	μ GPa	V_p km s^{-1}	V_s km s^{-1}	θ_D K
300	3.597±0.006	0.736	167.77±0.71	166.6±0.7	106.94±0.17	9.289±0.011	5.453±0.004	824±1
350	3.593	0.808	166.98	165.5	106.34	9.270	5.440	822
400	3.589	0.865	166.24	164.4	105.72	9.252	5.427	820
450	3.585	0.910	165.53	163.4	105.09	9.234	5.414	818
500	3.581	0.945	164.90	162.5	104.46	9.217	5.401	816
550	3.576	0.973	164.31	161.6	103.82	9.201	5.388	813
600	3.571	0.995	163.29	160.3	103.12	9.177	5.373	811
650	3.567	1.013	162.28	159.0	102.45	9.154	5.359	808
700	3.562	1.028	161.63	158.1	101.79	9.137	5.346	806
750	3.557	1.041	161.09	157.2	101.13	9.121	5.332	804
800	3.552±0.007	1.052	160.31±1.02	156.2±1.0	100.45±0.19	9.101±0.019	5.318±0.005	801±1
850	3.547	1.065	159.58	155.2	99.78	9.082	5.304	799
900	3.542	1.072	158.93	154.3	99.08	9.064	5.289	796
950	3.537	1.082	158.08	153.2	98.40	9.043	5.274	794
1000	3.532	1.092	157.49	152.3	97.69	9.026	5.256	791
1050	3.527	1.102	156.89	151.5	97.02	9.008	5.245	789
1100	3.522	1.113	156.22	150.6	96.35	8.991	5.230	786
1150	3.517	1.126	155.25	149.4	95.63	8.967	5.215	783
1200	3.512	1.139	154.35	148.3	94.88	8.943	5.198	780
1250	3.506	1.154	153.37	147.2	94.14	8.918	5.182	778
1300	3.501±0.008	1.170	152.58±1.20	146.2±1.2	93.41±0.21	8.897±0.020	5.165±0.006	775±1
1350	3.496	1.188	152.05	145.5	92.70	8.880	5.149	772

T: Temperature. ρ: Density. C_P: Specific heat capacity at constant pressure. K_S and K_T: Adiabatic and isothermal bulk (isotropic) moduli. μ: Isotropic shear modulus. V_p and V_s: Isotropic compressional and shear wave velocities. θ_D: Debye temperature
[a] Krupka et al. (1979)

tives reported on other garnets at 300 K (Table 5). The results given in Tables 4 and 5 for specimens GR-2B and GGD are found by fitting in a least squares procedure the primary data (Figs. 2–6; Tables 3a, b), to a first or second order Taylor series given by

$$M(T)=M_{300}+\left(\frac{\partial M}{\partial T}\right)_{300}(T-300\,K)+\frac{1}{2}\left(\frac{\partial^2 M}{\partial T^2}\right)_{300}(T-300\,K)^2. \quad (12)$$

Table 4. Elastic Properties of Calcium-Rich Garnets (300 K)

	GR-2B[a]	GR-2B[b]	GR-2B(cal)[c]	GGD[a]	GGD(cal)[c]	Bass [1989][d]	Bass [1989][e]
ρ	3.667(0.003)	3.667(0.003)	3.661[6]	3.597(0.005)	3.602[f]	3.602(0.036)	3.594[6]
C_{11}^S				318.8(0.8)	318(2)	321.7(0.8)	319(2)
C_{12}^S				92.1(0.7)	95(5)	91.4(0.9)	95(3)
C_{44}^S				102.9(0.2)	103(1)	104.6(0.4)	103(1)
C_S				113.4(0.3)	112(3)	115(1)	112(4)
K_S	166.2(1.2)	164.0(1.6)	167(2)	167.8(0.7)	170(2)	168.4(0.7)	170(2)
K_T	165(1)			166.4(0.7)			
μ	103.4(0.2)	103.4(0.3)	103(1)	107.0(0.2)	106(1)	108.9(0.4)	107(1)
V_p	9.10(0.02)	9.07(0.03)	9.12(0.04)	9.29(0.01)	9.30(0.04)	9.33(0.01)	9.33(0.04)
V_s	5.310(0.006)	5.30(0.01)	5.30(0.03)	5.452(0.004)	5.42(0.03)	5.50(0.01)	5.46(0.03)

ρ (gm cm^{-3}). C_{ij}^S, C_S, K_S, K_T, and μ (GPa). μ calculated from average of Hashin-Shtrikman (1962) upper and lower bounds. $V_{p,s}$ (km s^{-1}), where errors are propagated from K_S, μ, and ρ

[a] Present results. Errors in elastic moduli include s.d. of modal frequencies, uncertainties due to ρ, and the upper and lower bounds in Hashin-Shtrikman average, where applicable

[b] Babuska et al. (1987)

[c] Calculated from endmembers: grossular and spessartine (Bass 1989); andradite (Bass 1986); pyrope and almandine (Isaak and Graham 1976)

[d] Data on 99% grossular (Bass 1989)

[e] End member grossular from regression analysis of Bass (1989)

[f] Calculated from data of Skinner (1956)

Table 5. Temperature Variation of the Elastic Properties of Garnets at 300 K

	GR-2B[a]	GGD[a]	Py/Alm[b]	Py[c]	Alm[d]	Alm/Sp[e]
$(\partial C_{11}^S/\partial T)_P$		−3.61	−3.60	−3.34	−4.07	−3.33
$(\partial^2 C_{11}^S/\partial T^2)_P$		−3.8				
$(\partial C_{12}^S/\partial T)_P$		−0.33	−1.11	−1.48	−1.11	−0.91
$(\partial^2 C_{12}^S/\partial T^2)_P$		–				
$(\partial C_{44}^S/\partial T)_P$		−1.02	−0.80	−0.60	−1.22	−0.87
$(\partial^2 C_{44}^S/\partial T^2)_P$		−2.0	−1.9			
$(\partial C_S/\partial T)_P$		−1.63	−1.17	−0.93	−1.48	−1.21
$(\partial^2 C_S/\partial T^2)_P$		−2.1	−2.0			
$(\partial K_S/\partial T)_P$	−1.47(2)	−1.49(1)	−1.94	−2.10	−2.10	−1.72
$(\partial^2 K_S/\partial T^2)_P$	−1.8(2)	–				
$(\partial K_T/\partial T)_P$	−2.09(2)	−2.00(1)	−2.56			
$(\partial^2 K_T/\partial T^2)_P$	–	–				
$(\partial \mu/\partial T)_P$	−1.25(1)	−1.25(1)	−0.93	−0.73	−1.32	−1.00
$(\partial^2 \mu/\partial T^2)_P$	−1.1(1)	−2.1(1)	−2.3			
$(\partial V_p/\partial T)_P$	−0.035(1)	−0.035(1)	−0.038			
$(\partial^2 V_p/\partial T^2)_P$	−0.06(1)	−0.07(2)	−0.03			
$(\partial V_s/\partial T)_P$	−0.026(1)	−0.025(1)	−0.020			
$(\partial^2 V_s/\partial T^2)_P$	−0.04(1)	−0.07(1)	−0.03			

Indicated errors in parentheses represent standard deviations of weighted fits of isotropic data to first (or second) order polynomial. Uncertainty in last significant digit only is shown

First derivative units are (10^{-2} GPa K^{-1}) and (10^{-2} km s^{-1} K^{-1})

Second derivative units are (10^{-6} GPa K^{-2}) and (10^{-6} km s^{-1} K^{-2})

[a] Present results

[b] Pyrope (74%) – almandine (16%) (Suzuki and Anderson 1983)

[c] Estimated pyrope endmember (Sumino and Nishizawa 1978)

[d] Estimated almandine endmember (Sumino and Nishizawa 1978)

[e] Almandine (52%) – spessartine (46%) (Isaak and Graham 1976)

The M_{300}, $(\partial M/\partial T)_{300}$, and $(\partial^2 M/\partial T^2)_{300}$ coefficients are those given in Tables 4 and 5 for C_{ij}^S, K_S, K_T, μ, V_p, and V_s for GR-2B and GGD.

For GR-2B we find $K_S = 166.2 \pm 1.2$ GPa, which is higher than the value of 164.0 ± 1.6 reported by Basbuska et al. (1978) on this same specimen (Babuska et al. (1978) results are also shown in Table 4). This needs to be explained, in spite of the overlap in error bars, since these measurements were on the same specimen using the same technique. Babuska et al. (1978) used 15–25 resonance frequencies in determining the C_{ij}^S of a variety of garnets, but do not state how many frequencies were used with specimen GR-2B. In our work we used all of the lowest 37 modal frequencies. While increasing the

number of modal frequencies does not significantly alter the computed values of K_S and μ, it does lower the standard deviation of the calculated moduli. We note that in the lowest 20 modal frequencies there are four modes (B1u-01, B3u-01, B3u-02, B3g-02) for which the measured resonance frequencies have relatively large deviations from the final computed values. When we recompute the C_{ij}^S using the lowest 20 modal frequencies, with the exception of these four, we obtain $K_S = 164.8 \pm 1.6$ GPa, which is close to that reported by Babuska et al. (1978). Presumably, this approach was used by Babuska et al. (1978). In our final analysis we retained these frequencies, using all of the 37 lowest modes at each temperature.

We note that if our value of $K_S = 166.2$ GPa is more representative of that for a grossular-andradite garnet with GR-2B composition than is 164.0 GPa reported by Babuska et al. (1978), then K_S for this composition lies on the linear join from the endmembers grossular to andradite (see Fig. 2 of (O'Neill et al. 1989)), provided the lower value for K_S of 168.4 GPa (Bass 1989) is used for endmember grossular in that figure. The value of 168.4 GPa, rather than 171.4 GPa from the data of Halleck (1973), is consistent with our GGD K_S result as well. This observation implies that a linear relationship between K_S and modal grossular content in the grossular-andradite solid solution series adequately describes the situation for 76% grossular. However, data at other molar ratios on this join, particularly at 70% andradite (Babuska et al. 1978), suggest a linear mixing ratio on this join does not describe the values of K_S for intermediate compositions (Bass 1986; O'Neill et al. 1989).

By comparing columns 4 and 7 in Table 4 it is apparent that the values we find for GGD at 300 K are indistinguishable from the grossular endmember elastic moduli calculated from a regression analysis of the other available data to date (Bass 1989). We also list in Table 3 (column 5) the calculated elastic moduli for a garnet with the same chemistry as GGD from the endmember values given by Bass (1989) for grossular and spessartine, Bass (1986) for andradite, and Isaak and Graham (1976) for pyrope and almandine. The differences between columns 4 and 5 of Table 4 are slight and within the overlap of errors. On the other hand there are some small differences (outside the error overlap) between the nearly pure grossular data of Bass (1989), given in column 6 of our Table 4, and the calculated endmember grossular C_{44} and μ. But these differences are only about 1–2%, and we generally confirm the endmember grossular data of Bass (1989). In particular we note that the C_{12}^S and K_S moduli found in both our measurements and those of Bass (1989) suggest that these two moduli are lower by about 3% (C_{12}^S), and 2% (K_S), than found from the regression analysis, although the the error bars overlap.

The derivatives listed in Table 5 show that there are no essential differences between GGD and GR-2B in the 300 K temperature derivatives of the bulk properties, K_S, K_T, μ, V_p, and V_s. This result implies that the substitution of Fe for Al in the Y_2^{+3} site has negligible effect on the temperature dependences of the elastic moduli, which may not be too surprising in view of the similarities in radii of the Al and Fe ions. However the temperature variation of elasticity is a higher order effect, and to date no simple systematics adequately explains the relationship between this temperature dependence and atomic radii in a solid solution.

It is also evident from Table 5 that the inclusion of Ca in the divalent X_3^{+2} site in the garnet solid solution series has different effects on $(\partial K_S/\partial T)_P$, compared to $(\partial \mu/\partial T)_P$. Our data show that the presence of calcium tends to lower $|(\partial K_S/\partial T)_P|$ and to increase $|(\partial \mu/\partial T)_P|$ when these derivatives are compared to those of other garnets. Our temperature derivative for K_S is the smallest in absolute value of any derivative data found to date on garnets. Comparing our values for $(\partial K_S/\partial T)_P$ with that of almandine (Table 5) show significant changes in this derivative when substituting Ca for Fe in the X_3^{+2} site, which is in contrast to Al–Fe interchanging in the Y_2^{+3} as discussed above. In contrast, the relatively large value we find for $|(\partial \mu/\partial T)_P|$ is comparable to that of endmember almandine estimated by Sumino and Nishizawa (1978), but greater than for all other garnets.

We find that for most of the physical properties included in Table 5 there is a small, but measurable, nonlinear effect over the ranges of temperatures we used. The coefficients $(\partial M/\partial T)_{300}$ and $(\partial^2 M/\partial T^2)_{300}$, where appropriate, from (12) are shown in Table 5. There is too much scatter in the K_S data for specimen GGD to warrent a second order fit in temperature T. We find the second order temperature derivatives of K_S for GR-2B, and of μ, V_p, and V_s for both GGD and GR-2B to be a little smaller in magnitude, but with the same sign as found by Isaak et al. (1989) in their high temperature elasticity data for forsterite. The effect of the largest second order term in Table 5 from our data, that of $(\partial^2 \mu/\partial T^2)_P$ for GGD, is to decrease μ by about 3 GPa when using it to extrapolate from 300–1900 K in (12). It is worth noting that for GR-2B the average values of $(\partial K_S/\partial T)_P$ and $(\partial \mu/\partial T)_P$ over the entire 300–1250 K range in temperature are -0.0156 and -0.0130 GPa K^{-1}, respectively, which compare with the preliminary values of -0.0159 and -0.0145 reported by Isaak and Anderson (1987) over a more limited temperature range on this specimen. We prefer our present values because of the better modal sampling described above, and because in the earlier work of Isaak and Anderson (1987) lithium niobate transducers were used in order to withstand the high temperatures. Lithium niobate transducers produce several sharp resonant modes which are difficult to distinguish from those due to the specimen, and some incorrect identifications of frequencies are possible. In the present experiment we used apparatus equipped with buffer rods and thus were able to use lead zirconium-titanate transducers for which this effect is absent.

Discussion

Dimensionless Parameters and Elastic Thermal Equations of State

Dimensionless parameters related to the temperature derivatives of K_S, K_T, and μ have assumed important roles

Table 6a. Dimensionless Parameters for Grossular-Andradite Garnet (GR-2B)

T(K)	δ_S	δ_T	Γ	γ	$\delta_T-\delta_S$	ν
300	4.37	6.18	5.97	1.25	1.81	1.24
400	3.84	5.38	5.24	1.22	1.54	1.23
500	3.65	5.07	4.96	1.19	1.42	1.23
600	3.55	4.90	4.84	1.18	1.35	1.23
700	3.53	4.82	4.80	1.17	1.29	1.23
800	3.51	4.76	4.79	1.16	1.25	1.22
900	3.53	4.74	4.81	1.15	1.21	1.22
1000	3.56	4.74	4.84	1.14	1.18	1.22
1100	3.58	4.74	4.88	1.13	1.16	1.22
1200	3.61	4.74	4.93	1.11	1.13	1.22
	±0.10	±0.10	±0.1	±0.05	±0.14	±0.05

$\delta_S=-(1/\alpha K_S)(\partial K_S/\partial T)_P$
$\delta_T=-(1/\alpha K_T)(\partial K_T/\partial T)_P$
$\Gamma=-(1/\alpha\mu)(\partial\mu/\partial T)_P$
Grüneisen parameter, $\gamma=(\alpha K_S)/(\rho C_P)$
$\nu=(\partial \ln V_s/\partial \ln V_p)_P$

Table 6b. Dimensionless Parameters for Grossular Garnet (GGD)

T(K)	δ_S	δ_T	Γ	γ	$\delta_T-\delta_S$	ν
300	4.63	6.28	6.09	1.22	1.65	1.22
400	3.92	5.36	5.27	1.22	1.44	1.23
500	3.63	4.97	4.96	1.21	1.34	1.24
600	3.50	4.80	4.87	1.20	1.30	1.25
700	3.40	4.69	4.83	1.19	1.29	1.26
800	3.34	4.63	4.85	1.19	1.29	1.27
900	3.31	4.60	4.90	1.19	1.28	1.28
1000	3.30	4.58	4.96	1.18	1.29	1.29
1100	3.27	4.57	5.04	1.17	1.30	1.30
1200	3.25	4.56	5.10	1.14	1.31	1.31
1300	3.26	4.58	5.21	1.12	1.32	1.32
	±0.10	±0.10	±0.10	±0.05	±0.14	±0.05

$\delta_S=-(1/\alpha K_S)(\partial K_S/\partial T)_P$
$\delta_T=-(1/\alpha K_T)(\partial K_T/\partial T)_P$
$\Gamma=-(1/\alpha\mu)(\partial\mu/\partial T)_P$
Grüneisen parameter, $\gamma=(\alpha K_S)/(\rho C_P)$
$\nu=(\partial \ln V_s/\partial \ln V_p)_P$

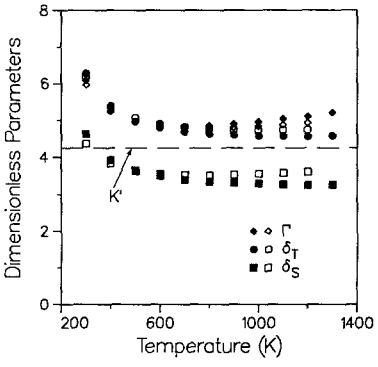

Fig. 7. Dimensionless parameters δ_S, δ_T, and Γ for garnet specimens GGD and GR-2B. The GGD data are those which extend to 1300 K (*solid symbols*), and the GR-2B data are represented by the *open symbols*. The parameter K' is $(\partial K/\partial P)_T$ at ambient conditions

in attempts to define systematics which can provide reasonable estimates of elastic properties at elevated pressure and temperature conditions. Furthermore dimensionless parameters have been used to extrapolate elasticity measurements made at low temperatures, to temperatures more representative of those in Earth's upper and lower mantle. A recent example is the work of Duffy and Anderson (1989).

We have tabulated several dimensionless parameters in Tables 6a, b for each of the specimens GR-2B and GGD. Figure 7 shows the temperature variations of δ_X defined by

$$\delta_X=-\left(\frac{1}{\alpha K_X}\right)\left(\frac{\partial K_X}{\partial T}\right)_P=\left(\frac{\partial \ln K_X}{\partial \ln \rho}\right)_P \tag{13}$$

where X is either S or T for the adiabatic and isothermal cases, respectively. The temperature dependence of the dimensionless quantity Γ is also illustrated in Fig. 7, where Γ is similar in form to δ_X and is defined by

$$\Gamma=-\left(\frac{1}{\alpha\mu}\right)\left(\frac{\partial\mu}{\partial T}\right)_P=\left(\frac{\partial \ln\mu}{\partial \ln\rho}\right)_P. \tag{14}$$

From Fig. 7 we observe a feature of the temperature variations of δ_S, δ_T, and Γ which has also been found for other minerals for which high temperature thermoelastic data are available. This feature is that for $T>\theta_D$ each of δ_S, δ_T, and Γ are nearly independent of temperature. This is not the case at lower temperatures since each of δ_S, δ_T, and Γ increase by 20–30% as temperature is lowered from 800 to 300 K, where 800 K is the approximate Debye temperature. The amount by which these dimensionless parameters increase as temperature is lowered from θ_D to 300 K is generally comparable to, and in most cases slightly larger than found over a similar temperature range for other oxide and silicate minerals: corundum (Goto et al. 1989); forsterite (Isaak et al. 1989a); Fe-bearing olivine (Isaak 1992); MgO (Isaak et al. 1989b); and CaO (Oda et al. 1992). The temperature independence of these dimensionless parameters is not exact for high T. We find, for example, that Γ for GGD increases slightly as temperature increases from 800–1300 K, albeit by less than 10%.

We note the close correspondence of δ_T and Γ observed in the grossular data from Fig. 7. This is also seen in the high temperature olivine and forsterite data (Isaak 1992; Isaak et al. 1989a), but for pyrope Γ at elevated temperature is about 20% lower than δ_T. A further empirical observation is that for grossular, the pressure derivative $(\partial K_S/\partial P)_T=K'_0$ at ambient conditions is 4.25 (Halleck 1973), which lies just below the high temperature grossular δ_T and Γ values. In the case of pyrope $K'_0=4.7$ (Bonzcar et al. 1977) which is only 0.4 higher than $\Gamma=4.3$ at high T. Thus the idea that the ambient K'_0 tends to be lower bound on Γ at the high temperature is true for grossular, and approximately true for pyrope. Isaak (1992) showed that if K'_0 also acts as a lower bound for Γ in β-phase olivine then the 400-km shear wave discontinuity in Earth's mantle requires about 46% olivine.

One reason accurate information on the temperature variations of δ_S, δ_T, and Γ are important is because these parameters can be used to extrapolate the elastic moduli to temperatures beyong the range of measurements. Equation (12) should be viewed essentially as an interpolative description of the temperature dependences of M over the range for which data were retrieved. It is generally assumed that nonlinear polynomial forms lead to unreliable values when extrapolated beyond the temperature range of measurements. An alternative approach is to integrate (13) and (14) thereby obtaining

$$\frac{M(T)}{M(T_0)} = \left[\frac{\rho(T)}{\rho(T_0)}\right]^{\{M\}_P} \tag{15}$$

where $M(T)$ and $M(T_0)$ represent K_S, K_T, or μ at elevated and room temperatures, respectively. The quantity $\{M\}_P$ is the corresponding δ_S, δ_T, or Γ for when M is K_S, K_T, or μ, respectively, as in the notation adopted by D.L. Anderson (1988) and Duffy and D.L. Anderson (1989).

Figures 8a, b illustrate the extrapolations of K_S and μ for grossular GGD to 2000 K under different assumptions. For comparison we also show similar extrapolation plots for forsterite (see Fig. 8c, d) which are taken from the data of Isaak et al. (1989a). Each plot, except for K_S of GGD, shows both a linear and a second order Taylor series representation of K_S or μ against T. For K_S of GGD only a linear term is used. The $(\partial^2 M/\partial T^2)_P$ terms used to draw the K_S and μ curves for forsterite are those found by Isaak et al. (1989a) over the range 300–760 K. Also illustrated in these plots are the temperature variations found in K_S and μ when (15) is used, with the $\{M\}_P$ values (i.e., δ_S or Γ) being those at 300 K, and then at θ_D. It is apparent that the θ_D values of $\{M\}_P$, together with (15), give a much better representation of the high temperature moduli where data are available, than do the low temperature values of $\{M\}_P$. The decreases found for both δ_S and Γ as temperature increases from 300 K to θ_D are about twice as great for GGD than for forsterite. For this reason the discrepancies between the extrapolations using (15) with $\{M\}_P$ at low, and then high temperature, are more significant for grossular than for forsterite (see Fig. 8a–d). The ranges in the estimated K_S and μ at 2000 K for GGD are 9 and 5 GPa, respectively, or 20–25% of the total change due to temperature, when low and high T $\{M\}_P$ are used in (15). This magnitude of uncertainty is cited by Duffy and Anderson (1989) in their extrapolations to high temperature, but we conclude that in cases for which data are available to θ_D the uncertainty can be reduced.

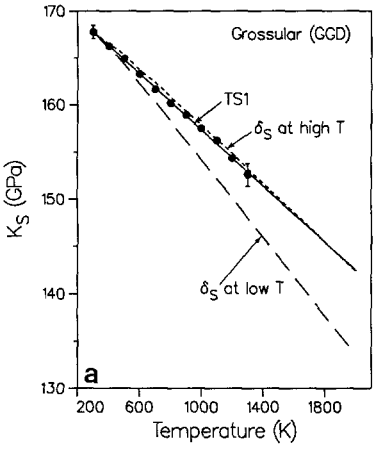

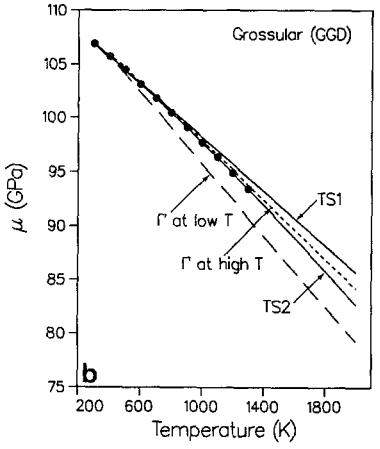

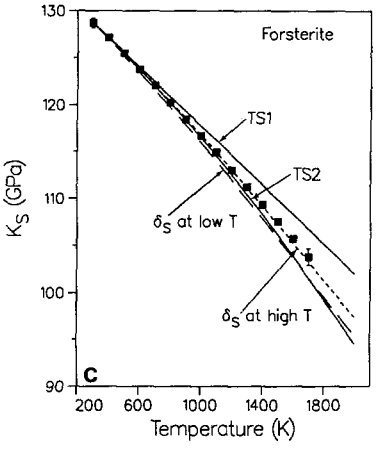

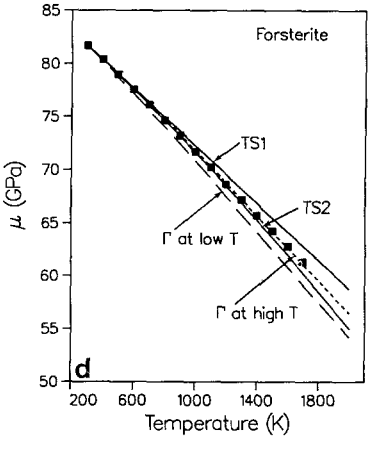

Fig. 8. Extrapolations of K_S and μ to 2000 K. **a**, **b** show results for grossular (GGD), and **c**, **d** show forsterite (Isaak et al. 1989a). TS1 and TS2 refer to first and second order Taylor series expansions (12), using coefficients in Table 5. The *long dashed lines* are found using (15) with the value of $\{M\}_P$ (i.e., δ_S or Γ) at $T=300$ K. The *short dashed lines* are found using the value of $\{M\}_P$ at $T=\theta_D$ in (15). The TS2 lines for forsterite are constructed using the $(\partial^2 M/\partial T^2)_P$ coefficients found for $300<T<760$ K (Isaak et al. 1989a)

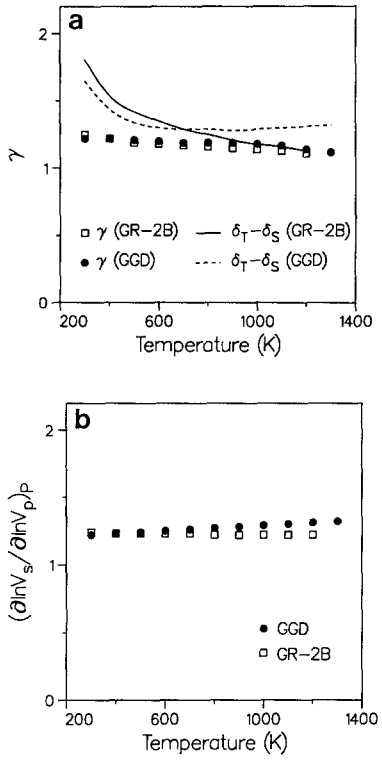

Fig. 9a, b. Dimensionless parameters: **a** Grüneisen parameter, γ, and **b** $\nu=(\partial \ln V_s/\partial \ln V_p)_P$ at ambient pressure. Included in (a) are $\delta_T-\delta_S$, showing their near equivalence to γ

Both Anderson (1989) and Sumino et al. (1983) suggested alternative methods by which to extrapolate K_S to temperatures beyond those measured. The method of Anderson (1989) was to demonstrate that K_S is linearly dependent on enthalpy for the minerals he investigated, and then to use enthalpy data which are generally available at higher temperatures, to obtain K_S. Sumino et al. (1983) suggested using the idea that at some high temperature T_r, which they took to be θ_D, that for $T>T_r$ the Grüneisen parameter γ is approximately independent of temperature. Thus K_S at high temperature is obtained by using the γ found at T_r in (8), along with the α, ρ, and C_P values appropriate to the high T. We note that both of these methods are applicable only to extrapolating K_S, but not μ. We emphasize that the method of Sumino et al. (1983) can be applied only when the temperature independence of γ for $T>T_r$ is confidently known. Figure 9a illustrates the slight decrease in γ with increasing T, found for both specimens GR-2B and GGD for $T>\theta_D$. For GGD the decrease in γ is about 7% as temperature increases from 800 K ($\approx\theta_D$) to 1300 K. This implies that K_S is overestimated by 7% at 1300 K, if the value of γ at 800 K is assumed for $T=1300$ K. This 7% overestimate in K_S at 1300 K is more than the total 5% decrease observed in K_S from 800–1300 K.

We have included the dimensionless parameter ν defined by

$$\nu=\left(\frac{\partial \ln V_s}{\partial \ln V_p}\right)_P \tag{16}$$

in Tables 6a, b, and illustrate the fact that this parameter is considerably less than 2.0, being approximately constant, with increasing temperature (Fig. 9a). These results are similar to those found for other high temperature measurements on oxides and silicates; specifically that the ambient pressure value of ν is approximately independent of T, and lies between 0.9 and 1.5. This is in contrast to seismic evidence that ν is 2.0–2.5 in the lower mantle. Discussions regarding possible interpretations of this discrepancy are found in Duffy and Ahrens (1991), Agnon and Bukowinski (1990) and Isaak et al. (1992), in addition to the possibility not yet discounted that unmeasured high-pressure phases have temperature dependences of wave velocities for which ν is 2.0–2.5.

Systematics and K_S Within the Garnet Solid Solution Series

Attempts to define systematic relationships between ρ, m, K_S, and μ among minerals are motivated by a desire to estimate elastic properties of unmeasured minerals. As it turns out an excellent approximation found from observation is that K_S is constant within the garnet solid solution series. This observation regarding K_S in the garnet solid solution also follows from the following approximation (Anderson 1988) relating the variation of K_{S_0} with ρ_0 for a given structure

$$V_\phi=A\rho^{-1/2} \tag{17}$$

in a solid solution, where $V_\phi=(K_S/\rho)^{1/2}$ and A is an integrating constant. Equation (17) is itself an approximation of the systematic relationship (Shankland 1972)

$$\left(\frac{\partial \ln V_\phi}{\partial \ln m}\right)_X=-\frac{1}{2} \tag{18}$$

and is discussed by Anderson (1988). Equation (18) describes how V_ϕ changes with average atomic mass at $X=$constant crystal class. The essential point is that within the garnet solid solution series the approximation represented by (17) coincides quite well with the observed lack of variation in K_S for the garnet solid solution. The constancy of K_S occurs because substituting a heavy cation increases both m and ρ in such a way that K_S is not affected significantly as can be seen from (18). If the lattice is significantly distorted by the substitution of a large ion, then X is not constant and slight deviation in K_S can occur.

In Table 7 we list K_S and μ for end member garnets, and include the recent Brillioun data on garnets with majorite components (Bass and Kanzaki 1990; Yeganeh-Haeri 1990). A simple average of K_S for the four pyralspites in Table 7 is 174 ± 4 GPa, and when the andradite and uvarovite garnets are included this average is 169 ± 8 GPa. These average values are within the range of measured values, 164–172 GPa, for the majorite-bearing garnets listed in Table 7, given the uncertainty in the majorite data. Earlier results of Yagi et al. (1987)

Table 7. Isotropic Elastic Moduli of Garnets

Pyralspite garnets	ρ	K_S	μ	ref.
grossular	3.618	169(1)	105(1)	1
spessartine	4.187	174(1)	95(1)	1
almandine	4.321	178(1)	97(1)	1
pyrope	3.548	173(1)	92(1)	1
andradite	3.836	157(2)	90(1)	2
uvarovite	3.850	162(2)	92(1)	2
Majorite garnets				
$Mj_{41}-Py_{59}$	3.555	164(15)	89(4)	3
$Mj_{66}-Py_{34}$	3.527	172(6)	92(4)	4
$Mj_{33}-Py_{67}$	3.545	170(15)	92(2)	4

[1] Babuska et al. (1978)
[2] Bass (1986)
[3] Bass and Kanzaki (1990)
[4] Yeganeh-Haeri et al. (1990)

($K_T = 164 \pm 1$ GPa for $Py_{42}-Mj_{58}$, where K_T is about 1 GPa lower than K_S at 300 K) using cubic-anvil high pressure apparatus are also nearly within the uncertainty of the simple assumption discussed above, although Yagi et al. had to assume what seems to be a low value of $K_0' = 2.0$ in their preferred data reduction. The majorite K_T value of 221 GPa found by Jeanloz (1981) is high in comparison to these data, and when viewed against these simple systematics. Given the current resolution of measurements on pyrope-majorite garnets, it is not yet possible to resolve the effect of x on Py_x-Mj_{1-x} along this join.

It is interesting that more involved systematics do not more accurately predict K_S for majorite garnets. For instance the seismic equation of state of D.L. Anderson (1967) has been reevaluated by Bass (1986) regarding its applicability to the garnet solid solution series. Bass (1986) found that with all the available garnet data a linear regression analysis yields

$$\ln \phi = 2.75 \ln\left(\frac{\rho}{m}\right) + 8.73 \tag{19}$$

where ϕ is K_S/ρ. In the original form of this expression, with a less complete data base, D.L. Anderson (1967) found the coefficient to be near 3.1, rather than 2.75. Application of (19) to estimate K_S for majorite gives a value of 191 GPa (Bass 1986), which is considerably higher than the Brillioun measurements in the range 164–172 GPa. Application of (18) also suggests the majorite K_S value is 191 GPa (Bass 1986). Thus the simple approximation of (17) seems to best describe the variability of K_S in the garnet solid solution series when the majorite components are also taken into account.

$(\partial K_S/\partial T)_P$ and $(\partial \mu/\partial T)_P$ Within the Garnet Solid Solution Series

Our results provide an expanded data base on the high temperature variation of K_S and μ in the garnet solid solution series. In particular our data shows that $|(\partial K_S/\partial T)_P|$ has a greater variation in the garnet solid solution series, than observed from previous temperature data on calcium-poor garnets. We also confirm that there is a significant variation in $|(\partial \mu/\partial T)_P|$ for garnet. This variation is due to chemical changes within an isomorphic mineral. The high value of $|(\partial \mu/\partial T)_P|$ for garnet in Table 5 is that predicted for almandine by Sumino and Nishizawa (1978), and is more than 80% larger than the low value, being that of pyrope. We emphasize that this high almandine $|(\partial \mu/\partial T)_P|$ value is an extrapolation out to almandine endmember composition from data retrieved on two garnet specimens, neither of which was more than 55% almandine. Our results are the first reported garnet measurements for which $|(\partial \mu/\partial T)_P|$ is larger than 1.1×10^{-2} GPa K^{-1}, and confirm the idea that there is large variation in this derivative due to chemical variation alone. Furthermore the chemical variation need not necessarily be that due to transitions metals. The differences spanned by K_S and μ at 1900 K due to extrapolating with the high and low $|(\partial M/\partial T)_P|$ derivatives from Table 5 are 10 and 8 GPa, respectively. These differences are significant and do not include effects of nonlinearity.

The only other high temperature ($T > \theta_D$) data available on a garnet are those of Suzuki and Anderson (1983) on pyrope-almandine. They found the values of δ_S, δ_T, and Γ at $T = \theta_D$ to be 4.1, 5.35, and 4.3, respectively, where we calculated Γ from their tabulated μ and α data since it was not include in their tables. The difference in δ_S between pyrope-almandine and grossular at 800 K is about 20%, and that in δ_T is about 15%. These compare to respective differences of 26 and 20% in $|(\partial K_S/\partial T)_P|$ and $|(\partial K_T/\partial T)_P|$ between grossular and almandine-pyrope. Thus the variation in these dimensionless derivatives are only slightly less than in $(\partial K_S/\partial T)_P$ and $(\partial K_T/\partial T)_P$ for the garnets on which high temperature data are available. On the other hand, since we find $\Gamma = 4.85$ at 800 K for grossular, the difference between this and Γ of pyrope-almandine is only about 12%, which is significantly smaller than the 30% difference in $(\partial \mu/\partial T)_P$. We conclude that the assumption that the dimensionless parameters δ_T, δ_S, and Γ are constant within the garnet solid solution has a firmer basis when tested against available high temperature data than assumptions regarding only the derivatives, $(\partial K_T/\partial T)_P$, $(\partial K_S/\partial T)_P$ and $(\partial \mu/\partial T)_P$, and more so the case for μ. Application of these ideas, using (15), to make quantitative estimates of K_S and μ for unmeasured garnet phases at high T require α data on the garnet phases of interest.

Since there is little variation in K_S within the garnet solid solution the preceding conclusion implies

$$\left(\frac{\partial K_S}{\partial T}\right)_{P,UM} \approx \left(\frac{\alpha_{UM}}{\alpha_M}\right)\left(\frac{\partial K_S}{\partial T}\right)_{P,M} \tag{20}$$

where M and UM represent measured and unmeasured garnet data, respectively. If $(\partial K_S/\partial T)_P$ is assumed constant, for example Duffy and Anderson (1989) adopt the $(\partial K_S/\partial T)_P$ value of garnet $Ca_3(Al, Fe)_2Si_3O_{12}$ for majorite $Ca_2Mg_2Si_3O_{12}$, then the assumption that α is approx-

imately equal in these two garnets is also implicitly made. More rigorous testing of this assumption requires α data on majorite garnets.

We note that (15) is an equivalent statement to (19) for $\{M\}_P=\delta_S$, if the variation of ϕ and ρ in (19) are due only to temperature for a given garnet composition. In this case the coefficient of 2.75 in (19) is identified with δ_S-1 from straightforward manipulation of (19). This means that $\delta_S=3.75$ from the best fit of all the available low pressure phase garnet data. It is of interest that this value also falls right between the δ_S obtained from our high temperature data on grossular and that of pyrope-almandine from Suzuki and Anderson (1983). Thus based on both high temperature elasticity data available to date, and on the systematics of the variation of ϕ and ρ for many non-majorite garnets, (15) with $M=K_S$ and $\{M\}_P=\delta_S=3.75$ is likely to give a good estimate of the temperature variation of K_S for any garnet provided that information on ρ at high temperature is also known.

It is worth noting the effect that high $(\partial\mu/\partial T)_P$ derivatives for Ca-rich garnets have on attempts to model the earth's transition zone velocity gradients. Bass and Kanzaki (1990) point out that Ca lowers the μ modulus of pyroxene, and increases μ of garnet, thus effectively increasing the contrast in μ from pyroxene to garnet at ambient conditions. If this contrast is maintained at elevated pressure and temperature, these authors note that large amounts of Ca-clinopyroxene would effectively satisfy the high transition zone velocity gradients. Our average value for $(\partial\mu/\partial T)_P$ of specimen GGD over the entire range of measurements is $-0.014\,\mathrm{GPa\,K^{-1}}$, which is larger in magnitude than $-0.010\,\mathrm{GPa\,K^{-1}}$ estimated for pyroxene (Duffy and Anderson 1989). If the grossular temperature derivative is somewhat representative of Ca-rich majorite then the difference in μ found between Ca-rich garnet and pyroxene at ambient conditions will be diminished by about 6 GPa, once temperature effects are accounted for. This smaller difference in μ at high T in turn would require even more pyroxene in the mantle, or further enrichment of Ca in the pyroxene, than the 2:1 ratio of diopside:enstatite and the 3:1 ratio of total pyroxene:garnet given as an example solution by Bass and Kanzaki (1990) to the shear velocity gradients in the transition zone.

Summary of Conclusions

1. We present new garnet thermal expansion data up to nearly 1000 K and find for grossular-andradite, what others have found for pyrope and almandine: the α data of Skinner (1956) seem to be 10–15% low.
2. Remeasurement of a grossular(76%)-andradite(22%) polycrystal shows that its room temperature value for K_S lies on the linear join between the endmembers grossular and andradite.
3. We obtain high quality elasticity data for a single-crystal near endmember grossular to 1350 K, and a polycrystalline grossular-andradite specimen to 1250 K. The polycrystalline data demonstrate the feasibility of retrieving accurate temperature data when single-crystal specimens are not available.
4. Calcium rich garnets generally have the lowest $|(\partial K_S/\partial T)_P|$ and among the highest $|(\partial\mu/\partial T)_P|$ values when compared with all other garnet temperature data. We find no essential difference in the temperature derivatives of K_S and μ for endmember grossular and grossular(76%)-andradite(22%). If the large magnitude of $|(\partial\mu/\partial T)_P|$ for grossular is also true for Ca-rich majorite garnets, then the difference in shear wave velocity between diopside and Ca-majorite diminishes as temperature is applied. This means that more Ca-enrichment of pyroxene and/or more total pyroxene is required if the high shear wave gradients in the transition zone are to be explained by a pyroxene to majorite transition.
5. We observe a small nonlinear temperature dependence in μ for both specimens which we measured, and nonlinearity in K_S for one specimen. The nonlinear temperature dependence is comparable to, but a little less than that found in forsterite. The most effective extrapolations for K_S and μ are those that utilize the values of dimensionless parameters δ_S and Γ taken at their Debye temperature.
6. The dimensionless parameters δ_S and Γ at high temperature show less variation within the garnet solid solution series than do the derivatives $(\partial K_S/\partial T)_P$ and $(\partial\mu/\partial T)_P$. This is a tentative conclusion since there are limited high temperature elasticity available for garnets, but if it holds it suggests that these parameters are more useful in predicting the temperature variations of K_S and μ for unmeasured high pressure mantle garnet phases, than systematics involving just $(\partial K_S/\partial T)_P$ and $(\partial\mu/\partial T)_P$.
7. Our data on Ca-rich garnets show that Γ is near δ_T, and that K_0' is near, but slightly lower than Γ. This relationship between K_0' and Γ is similar to most every other oxide and silicate for which data at high temperature have been retrieved, and suggests that K_0' may be a useful means by which to estimate lower bounds on Γ, and thereby constrain the magnitude of $|(\partial\mu/\partial T)_P|$.

Acknowledgments. We thank Jay Bass (Un. of Illinois at Urbana-Champaign) for giving us one of his fine single-crystal grossular specimens (GGD). Robert Jones (UCLA) gave invaluable assistance during the microprobe analysis of specimen GGD. Wayne Dollase (UCLA) provided use of x-ray equipment for orientating the single-crystal specimen, and Michael Mehl (Naval Research Laboratory) provided a helpful reading of the manuscript. This work was supported will NSF grant EAR8903928. IGPP contribution number 3653.

References

Agnon A, Bukowinski MST (1990) δ_S at high pressure and $d\ln V_S/d\ln V_P$ in the lower mantle. Geophys Res Lett 17:1149–1152

Anderson DL (1967) A seismic equation of state. Geophys J R Astron Soc 13:9–30

Anderson DL (1988) Temperature and pressure derivatives of elastic constants with application to the mantle. J Geophys Res 93:4688–4700

Anderson OL (1988) Simple solid-state equations for materials of terrestrial planet interiors. In: Runcorn SK (ed) The Physics of the Planets, pp 27–60. Wiley, New York

Anderson OL (1989) The relationship between the adiabatic bulk modulus and enthalpy for mantle-related minerals. Phys Chem Minerals 16:559–562

Babuska V, Fiala J, Kumazawa M, Ohno I, Sumino Y (1978) Elastic Properties of garnet solid-solution series. Phys Earth Planet Inter 16:157–176

Bass JD, Anderson DL (1984) Composition of the upper mantle: Geophysical tests of two petrological models. Geophys. Res. Lett. 11:237–240

Bass JD (1986) Elasticity of uvarovite and andradite garnets. J Geophys Res 91:7505–7516

Bass JD (1989) Elasticity of grossular and spessartite garnets by Brillioun spectroscopy. J Geophys Res 94:7621–7628

Bass JD, Kanzaki M (1990) Elasticity of a majorite-pyrope solid solution. Geophys Res Lett 17:1989–1992

Bonczar LJ, Graham EK, Wang H (1977) The pressure and temperature dependence of the elastic constants of pyrope garnet. J Geophys Res 82:2529–2534

Duffy TS, Ahrens TJ (1991) Sound velocities at high pressure and temperature and their geophysical implications. J Geophys Res (submitted)

Duffy TS, Anderson DL (1989) Seismic velocities in mantle minerals and the mineralogy of the upper mantle. J Geophys Res 94:1895–1912

Goto T, Anderson OL (1988) An apparatus for measuring elastic constants of single crystals by a resonance technique up to 1825 K. Rev Sci Instrum 59:1405–1408

Goto T, Anderson OL, Ohno I, Yamamoto S (1989) Elastic constants of corundum up to 1825 K. J Geophys Res 94:7588–7602

Gwanmesia GD, Liebermann RC, Guyot F (1990a) Hot-pressing and characterization of polycrystals of $\beta-Mg_2SiO_4$ for acoustic velocity measurements. Geophys Res Lett 17:1331–1334

Gwanmesia GD, Rigden S, Jackson I, Liebermann RC (1990b) Pressure dependence of elastic wave velocity for $\beta-Mg_2SiO_4$ and the composition of the earth's mantle. Science 250:794–797

Halleck PM (1973) The compression and compressibility of grossularite garnet: A comparison of X-ray and ultrasonic methods. Ph.D. Thesis University of Chicago, Chicago, Illinois, USA

Hashin Z, Shtrikman S (1962) A variational approach to the theory of the elastic behaviour of polycrystals. J Mech Phys Solids 10:343–352

Isaak DG, Graham EK (1976) The elastic properties of an almandine-spessartine garnet and elasticity in the garnet solid solution series. J Geophys Res 81:2483–2489

Isaak DG, Anderson OL (1987) The high temperature elastic and thermal expansion properties of a grossular garnet (abstract). Eos Trans AGU 68:410

Isaak DG, Anderson OL, Goto T, Suzuki I (1989a) Elasticity of single-crystal forsterite measured to 1700 K. J Geophys Res 94:5895–5906

Isaak DG, Anderson OL, Goto T (1989b) Measured elastic moduli of single-crystal MgO up to 1800 K. Phys Chem Minerals 16:704–713

Isaak DG (1992) High temperature elasticity of iron-bearing olivines. J Geophys Res 97:1871–1885

Isaak DG, Anderson OL, Cohen RE (1992) The relationship between shear and compressional velocities at high pressures: Reconciliation of seismic tomography and mineral physics. Geophys. Res. Lett. 19:741–744

Jeanloz R (1981) Majorite: vibrational and compressional properties of a high-pressure phase. J Geophys Res 86:6171–6179

Krupka KM, Robie RA, Hemingway BS (1979) High-temperature heat capacities of corundum, periclase, anorthite, $CaAl_2Si_2O_8$ glass, muscovite, pyrophyllite, $KAlSi_3O_8$ glass, grossular, and $NaAlSi_3O_8$ glass. Am Mineral 64:86–101

Leitner BJ, Weidner DJ, Liebermann RC (1980) Elasticity of single crystal pyrope and implications for garnet solid solution series. Phys Earth Planet Inter 22:111–121

Oda H, Anderson OL, Isaak GD (1992) Measurement of elastic properties of single crystal CaO up to 1200 K. Phys Chem Minerals (in press)

Ohno I (1976) Free vibration of a rectangular parallelepiped and its application to determination of elastic constants of orthorhombic crystal. J Phys Earth 24:355–379

O'Neill B, Bass JD, Smyth JR, Vaughan MT (1989) Elasticity of grossular-pyrope-almandine garnet. J Geophys Res 94:17819–17824

O'Neill B, Bass JD, Rossman GR, Geiger CA, Langer K (1991) Elastic properties of pyrope. Phys Chem Minerals 17:617–621

Papike JJ (1987) Chemistry of the rock-forming silicates: ortho, ring, and single-chain structures. Rev Geophys 23:1483–1526

Reddy PJ, Bhimasenachar J (1964) Temperature dependence of elastic compliances of garnet. Acta Crystallogr 17:31–32

Shankland TJ (1972) Velocity-density systematics: derivation from the Debye theory and the effect of ionic size. J Geophys Res 77:3750–3758

Skinner BJ (1956) Physical properties of end-members of the garnet group. Am Mineral 41:428–436

Soga N (1967) Elastic constants of garnet under pressure and temperature. J Geophys Res 72:4227–4234

Sumino Y, Ohno I, Goto T, Kumazawa M (1976) Measurement of elastic constants and internal friction on single-crystal MgO by rectangular parallelepiped resonance. J Phys Earth 24:263–273

Sumino Y, Nishizawa O (1978) Temperature variation of elastic constants of pyrope-almandine garnets. J Phys Earth 26:239–252

Sumino Y, Anderson OL, Suzuki I (1983) Temperature coefficients of elastic constants of single crystal MgO between 80 and 1300 K. Phys Chem Minerals 9:38–47

Suzuki I (1975) Thermal expansion of periclase and olivine, and their anharmonic properties. J Phys Earth 23:145–159

Suzuki I, Shin-ichi O, Seya K (1979) Thermal expansion of single-crystal manganosite. J Phys Earth 27:63–69

Suzuki I, Anderson OL (1983) Elasticity and thermal expansion of a natural garnet up to 1000 K. J Phys Earth 31:125–138

Touloukian YS, Kirby RK, Taylor RE, Lee TYR (eds) (1977) Thermophysical properties of matter, vol 13: Thermal expansion of nonmetallic solids. Plenum Press, New York

Wang H, Simmons G (1974) Elasticity of some mantle crystal structures 3. Spessartine-almandine garnet. J Geophys Res 79:2607–2613

Weaver JS, Takahashi T, Bass J (1976) Isothermal compression of grossular garnets to 250 kbar and the effect of calcium on the bulk modulus. J Geophys Res 81:2475–2482

Yagi T, Akaogi M, Shimamura O, Tamai H, Akimoto S (1987) High pressure and high temperature equations of state of majorite. In: Manghnani M, Syono Y (eds) High Pressure Research in Mineral Physics, pp 251–260. American Geophysical Union, Washington DC

Yeganeh-Haeri A, Weidner DJ, Ito E (1990) Elastic properties of the pyrope-majorite solid solution series. Geophys Res Lett 17:2453–2456